PRODUCTION AND HADRONIZATION OF HEAVY-FLAVOR HADRONS*

Min He

Department of Applied Physics, Nanjing University of Science and Technology
Nanjing 210094, China

Received 7 September 2022, accepted 14 October 2022,
published online 14 December 2022

An overview of selected recent theoretical developments of the production and hadronization of heavy flavor hadrons in nuclear collisions is presented. The presentation consists of three parts. The first part concerns the production of charm hadrons in high-energy proton–proton collisions. The second part describes the theoretical advancements in the determination of heavy-quark diffusion coefficient and hadronization mechanisms in the quark–gluon plasma (QGP) created in relativistic heavy-ion collisions. The third part reports on recent developments from modeling of heavy quarkonia production in heavy-ion collisions. While the first part serves as the baseline study for charm-hadron production in QGP, a close and quantitative connection between open- and hidden-charm transport in QGP as emerging from discussions in the second and third parts is revealed and highlighted.

DOI:10.5506/APhysPolBSupp.16.1-A22

1. Introduction

Heavy quarks, charm and bottom, have been used as a versatile tool of testing strong interactions, both in the perturbative and nonperturbative domains. For the former, heavy-quark masses being much larger than the $\Lambda_{\rm QCD}$ render their pairwise production ($c\bar{c}$ or $b\bar{b}$) calculable via perturbative QCD. In contrast, their hadronization takes place at a long timescale and requires nonperturbative modeling. High-energy proton–proton (pp) collisions and heavy-ion collisions (Pb–Pb) at the LHC energies provide new opportunities to study novel production and hadronization mechanisms of heavy flavor hadrons [1–6], in terms of both chemical and kinetic characteristics of open and hidden heavy flavors associated with multi-parton interactions in a hadronic medium (pp) or hot (QGP) and cold nuclear matter (CNM) effects (Pb–Pb). In these proceedings, we will present an overview of selected recent theoretical developments in these aspects.

* Presented at the 29th International Conference on Ultrarelativistic Nucleus–Nucleus Collisions: Quark Matter 2022, Kraków, Poland, 4–10 April, 2022.

2. Charm hadro-chemistry in high-energy *pp* collisions

The fragmentation functions (FFs) of heavy quarks have been typically parameterized from measurements in e^+e^- or ep collisions under the assumption that fragmentation of heavy quarks is universal across different colliding systems and energies [7]. Indeed such parameterizations have been successful in reproducing the charm-meson ratios, D^+/D^0 and D_s^+/D^0, in high-energy pp collisions [8]. However, the substantial enhancement of Λ_c^+/D^0 at low p_T as measured by the ALICE Collaboration in $\sqrt{s} = 5.02$ TeV at midrapidity relative to the value in e^+e^- collisions has posed a great challenge to the assumption of universal FFs [9], *cf.* Fig. 1. PYTHIA 8 with a tune that implements color reconnection topologies beyond the leading order approximation, in particular including junctions fragmenting into baryons, is able to reproduce the enhancement of the baryon production [10]. The Catania model assumes that a deconfined QGP droplet is formed and thus charm-quark hadronization occurs via coalescence with thermalized light quarks at low p_T [11], in the same manner as in Pb–Pb collisions [12]. The statistical hadronization model [13] was motivated by noting that in a light-quark-rich environment as created in high-energy pp collisions (unlike e^+e^- collisions), statistical coalescence of charm quarks with surrounding light quarks may become likely. Assuming *relative* chemical equilibrium among different charm-hadron species, statistical thermal densities were used as pertinent fragmentation weights of the charm quark into all possible kinds of charm hadrons. While the Λ_c^+/D^0 falls significantly short of ALICE data, if only charm hadrons as listed in the Particle Data Group (PDG) tables are incorporated in the statistical model calculation, it is much enhanced when

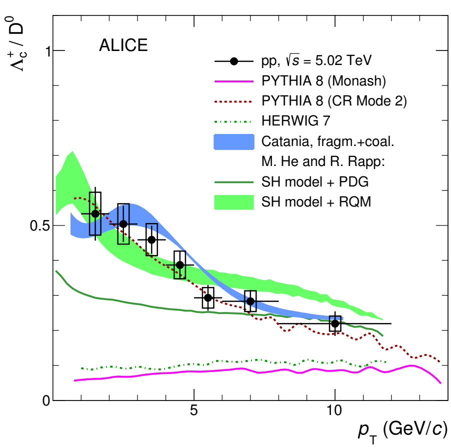

Fig. 1. The p_T dependence of Λ_c^+/D^0 ratios in $\sqrt{s} = 5.02$ TeV pp collisions. Figure adapted from [9].

the PDG list of charm-baryons were augmented by many more "missing" states taken from relativistic quark model (RQM) calculations [14], simply as a result of the feeddowns of the "missing" excited baryons into the ground state Λ_c^+.

The fragmentation fractions $f(c \to H_c)$, representing the probabilities of a charm quark to hadronizing into a given ground-state charm hadron specifies H_c, have been measured [15] and are roughly reproduced by the augmented statistical model calculations [13] as well as PYTHIA 8 with the new tune [10]. An overall feature is that charm content is significantly shuffled from the meson sector to the baryon sector [15] in high-energy pp collisions with respect to e^+e^- collisions. Since now all ground-state charm hadrons have been measured, a direct experimental value of total charm cross section in high-energy pp collisions has become accessible for the first time. The charm cross section per unit rapidity is $\mathrm{d}\sigma^{c\bar{c}}/\mathrm{d}y \sim 1165\ \mu$ b at mid rapidity in pp collisions at $\sqrt{s} = 5.02$ TeV [15], which is significantly higher than previous incomplete measurements and will have a significant impact on the theoretical modelling of charmonium transport in the QGP.

3. Charm interaction and hadronization in Pb–Pb collisions

3.1. Charm diffusion coefficient in the hot medium

Charm quark diffusion in the QGP can be simulated by the Fokker–Planck equation, which involves the charm-quark thermal relaxation rate $A(p,T)$ as a transport coefficient. The charm thermal relaxation rate, taken at the vanishing momentum limit, can be translated into the spatial diffusion coefficient via $\mathcal{D}_\mathrm{s} = T/(m_Q A(p=0,T))$ by dividing out the quark mass dependence in order to reflect the generic information of the medium. Figure 2 represents a summary of the status of theoretical calculations of $\mathcal{D}_\mathrm{s}$ in the unit of thermal wavelength. Calculations based on the quasiparticle Born scattering with an effective large coupling strength [16–18], strongly coupled solution within the nonperturbative lattice-constrained T-matrix approach [19, 20], and data-driven analysis [21] all suggest a small diffusion coefficient $\mathcal{D}_\mathrm{s}(2\pi T) \sim 2$–4 near T_c, a factor ~ 10 smaller than the LO-pQCD (with fixed $\alpha_\mathrm{s} \sim 0.3$) result. This is consistent with lattice QCD computations and also connects smoothly to the D-meson diffusion coefficient in the low-temperature hadronic phase [22, 23] as also shown in Fig. 2.

Recent precision measurements of D-meson R_{AA} and v_2 by the ALICE Collaboration also allow to extract the charm diffusion coefficient from the model-to-data comparison [24, 25]. The criterion for the selection of models by ALICE was the χ^2 per degrees of freedom being less than 5 for R_{AA} and less than 2 for v_2. The diffusion coefficient of $\mathcal{D}_\mathrm{s}(2\pi T) \sim 1.5$–4.5 near T_c used in the selected models thus represents a state-of-the-art extraction for this

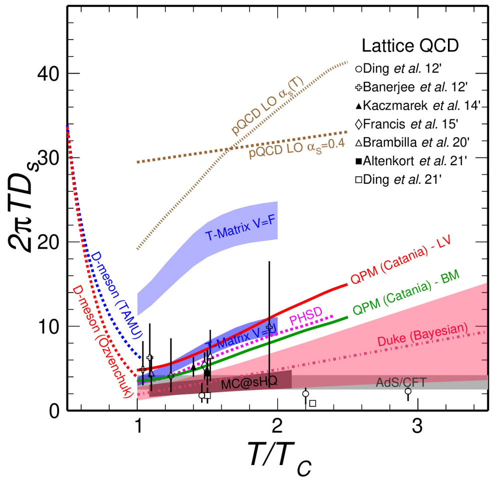

Fig. 2. The temperature dependence of charm spatial diffusion coefficient. Figure adapted from [5].

transport coefficient [24]. Such a small diffusion coefficient translates to a large scattering rate $\Gamma_{\rm coll} \sim 3/\mathcal{D}_{\rm s}$ of the order of 1 GeV, which is even greater than the light quark/gluon mass. This means that thermal partons must be already melted near the phase boundary but only heavy quarks survive. As revealed by the T-matrix approach, this strong coupling strength is probably caused by the significant remnants of confining force [20].

3.2. Charm hadronization and hadro-chemistry

The novel hadronization mechanism for charm quarks in the QGP is coalescence, which performs recombination of low-$p_{\rm T}$ charm quarks with thermal light quarks nearby in phase space and adds flow to the parent charm quark. At high $p_{\rm T}$, independent fragmentation into charm hadrons become dominant. Most heavy quark transport approaches employ the instantaneous model to perform the charm-quark coalescence [12, 26–28], which suffers from the drawback of energy nonconservation and thus does not have a controlled equilibrium limit that we believe is important for the formation of low-$p_{\rm T}$ charm hadrons. A recent improvement in this regard was to first form an off-shell excited cluster from the participating quarks and then decay it into an on-shell ground state [27, 29]. In contrast, energy is conserved and the equilibrium limit is satisfied [30] in the resonance recombination model (RRM) [31], by forming a resonance above the threshold using a resonant cross section. The RRM was recently generalized to the 3-body case by forming first a light diquark resonance and then the charm baryon one [32]. In this approach, the space-momentum correlations (SMCs) developed in the quark distributions through diffusion or hydrodynamics flow are incorporated, which are found to harden both the D^0 and Λ_c^+ p_T-spectra, more on the Λ_c^+, implying the enhancement of Λ_c^+/D^0 by this effect [32].

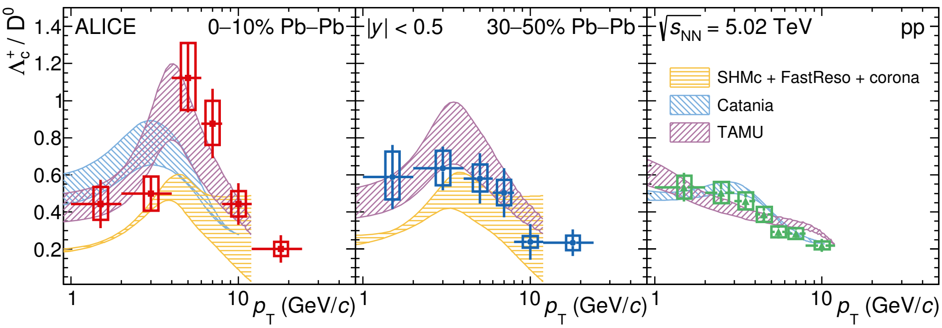

Fig. 3. The p_T dependence of Λ_c^+/D^0 ratios in $\sqrt{s_{NN}} = 5.02$ TeV Pb–Pb and *pp* collisions. Figure adapted from [33].

Recombination results in remarkable modifications in p_T-dependent charm hadro-chemistry, as mostly reflected in the Λ_c^+/D^0 ratio shown in Fig. 3, which demonstrates a significant enhancement at intermediate p_T especially in central collisions, and tends to the *pp* value at high p_T. Three model predictions are confronted with the data. The Catania model [12] based on instantaneous coalescence plus fragmentation overestimates (underestimates) the measured ratio at low (intermediate) p_T. The statistical hadronization model (SHMc) [34] that adopts PDG-only states and approximates the charm-hadron p_T-spectra by a hydrodynamic blast-wave (complemented with a *pp* spectra for the corona part) generally underpredicts the ratio. In contrast, both the magnitude and shape of the measured ratio are reproduced by the TAMU model [32] that adopts additional charm baryons from the RQM predictions as in *pp* collisions [13]. In this calculation, the enhancement of Λ_c^+/D^0 at intermediate p_T results from the RRM incorporating SMCs and capturing full flow effects. We also note that at low p_T, this ratio remains compatible with the value in *pp*, suggesting that the enhancement at intermediate p_T is primarily due to a kinematic redistribution of D^0 and Λ_c^+ in momentum space rather than additional charm-baryon production channels opening up in Pb–Pb collisions.

4. Quarkonia transport in Pb–Pb collisions

Semiclassical transport approaches based on the Boltzmann equations [35, 36] have shed great light on the charmonium production through dissociation and regeneration. However, these transport approaches have used a blast-wave spectrum for the charmonium regeneration component and predicted a J/ψ v_2 much below the ALICE measurement at intermediate p_T in Pb–Pb collisions [35, 36]. This was recently revisited by calculating the J/ψ regeneration via the RRM [37]. In particular, the state-of-the-art transported charm and anticharm quark spectra as constrained by open heavy flavor observables [32] implemented into the RRM [37]. The use of off-equilibrium charm and anticharm quark distributions (normalized to the state-of-the-art charm cross section [15] modulo charm shadowing) plus the incorporation of SMCs between them extend the reach of regeneration up to $p_T \sim 8$ GeV. As a result, the J/ψ v_2 is much enhanced with respect to previous calculations, as shown in Fig. 4. This highlights the importance of establishing a quantitative connection between open-charm and hidden-charm transport.

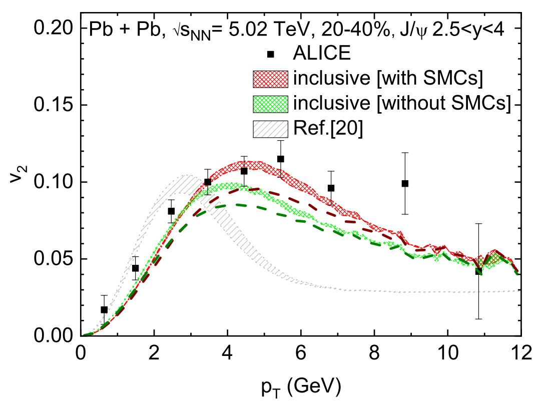

Fig. 4. The p_T dependence of inclusive J/ψ v_2 $\sqrt{s} = 5.02$ TeV Pb–Pb collisions in the 20–40% centrality class. The grey band indicates the result from a previous kinetic rate-equation approach using a blast-wave approximation [36]. Figure adapted from [37].

Open quantum system approaches within the framework of pNRQCD have been developed to tackle the production of bottomonia [38–40]. In this approach, quantum transitions between different states are included, which is lacking in semi-classical transport. Transport coefficients are encoded in the pertinent Lindblad equation [38], but regeneration is currently limited to the diagonal case. Experimental data of the R_{AA} and v_2 of $\Upsilon(1S)$ and $\Upsilon(2S)$ states have been well reproduced by this approach [38]. However, it is notable that the used transport coefficient, when translated into the Υ thermal width, turns out to be quite comparable to the values used in the semi-classical approach [41].

5. Summary

Heavy flavor particles are excellent probes of the structure, transport properties, in-medium force, and hadronization mechanisms of the sQGP. A small charm diffusion coefficient has been extracted, recombination as a color neutralization process has proved to play an important role in phenomenology, and quarkonia are being melted by large reaction rates — all these point to the emergence of a strong HQ potential, at least at temperatures not very far from T_{c}, suffering little screening and featuring significant remnants of confining force [20, 42]. This emerging picture then allows to establish a close connection between open- and hidden-charm transport, *e.g.* via J/ψ regeneration [37].

This work was supported by NSFC grant 12075122. The author acknowledges helpful discussions with Ralf Rapp.

REFERENCES

[1] A. Andronic *et al.*, *Eur. Phys. J. C* **76**, 107 (2016).
[2] X. Dong, Y.J. Lee, R. Rapp, *Annu. Rev. Nucl. Part. Sci.* **69**, 417 (2019).
[3] E. Chapon *et al.*, *Prog. Part. Nucl. Phys.* **122**, 103906 (2022).
[4] A. Rothkopf, *Phys. Rep.* **858**, 1 (2020).
[5] L. Apolinário, Y.J. Lee, M. Winn, *Prog. Part. Nucl. Phys.* **127**, 103990 (2022), arXiv:2203.16352 [hep-ph].
[6] M. He, H. van Hees, R. Rapp, arXiv:2204.09299 [hep-ph].
[7] E. Braaten, K.m. Cheung, S. Fleming, T.C. Yuan, *Phys. Rev. D* **51**, 4819 (1995).
[8] ALICE Collaboration (S. Acharya *et al.*), *Eur. Phys. J. C* **77**, 550 (2017).
[9] ALICE Collaboration (S. Acharya *et al.*), *Phys. Rev. Lett.* **127**, 202301 (2021).
[10] J.R. Christiansen, P.Z. Skands, *J. High Energy Phys.* **2015**, 003 (2015).
[11] V. Minissale, S. Plumari, V. Greco, *Phys. Lett. B* **821**, 136622 (2021).
[12] S. Plumari *et al.*, *Eur. Phys. J. C* **78**, 348 (2018).
[13] M. He, R. Rapp, *Phys. Lett. B* **795**, 117 (2019).
[14] D. Ebert, R.N. Faustov, V.O. Galkin, *Phys. Rev. D* **84**, 014025 (2011).
[15] ALICE Collaboration (S. Acharya *et al.*), *Phys. Rev. D* **105**, L011103 (2022).
[16] P.B. Gossiaux, J. Aichelin, *Phys. Rev. C* **78**, 014904 (2008).
[17] S.K. Das, F. Scardina, S. Plumari, V. Greco, *Phys. Lett. B* **747**, 260 (2015).
[18] T. Song *et al.*, *Phys. Rev. C* **92**, 014910 (2015).
[19] F. Riek, R. Rapp, *Phys. Rev. C* **82**, 035201 (2010).

[20] S.Y.F. Liu, M. He, R. Rapp, *Phys. Rev. C* **99**, 055201 (2019).

[21] Y. Xu *et al.*, *Phys. Rev. C* **97**, 014907 (2018).

[22] M. He, R.J. Fries, R. Rapp, *Phys. Lett. B* **701**, 445 (2011).

[23] L. Tolos, J.M. Torres-Rincon, *Phys. Rev. D* **88**, 074019 (2013).

[24] ALICE Collaboration (S. Acharya *et al.*), *J. High Energy Phys.* **2022**, 174 (2022).

[25] ALICE Collaboration (S. Acharya *et al.*), *Phys. Lett. B* **813**, 136054 (2021).

[26] Y. Oh, C.M. Ko, S.H. Lee, S. Yasui, *Phys. Rev. C* **79**, 044905 (2009).

[27] S. Cao *et al.*, *Phys. Lett. B* **807**, 135561 (2020).

[28] R. Katz *et al.*, *Phys. Rev. C* **102**, 024906 (2020).

[29] A. Beraudo *et al.*, *Eur. Phys. J. C* **82**, 607 (2022).

[30] M. He, R.J. Fries, R. Rapp, *Phys. Rev. C* **86**, 014903 (2012).

[31] L. Ravagli, R. Rapp, *Phys. Lett. B* **655**, 126 (2007).

[32] M. He, R. Rapp, *Phys. Rev. Lett.* **124**, 042301 (2020).

[33] ALICE Collaboration (S. Acharya *et al.*), `arXiv:2112.08156 [nucl-ex]`.

[34] A. Andronic *et al.*, *J. High Energy Phys.* **2021**, 035 (2021).

[35] K. Zhou, N. Xu, Z. Xu, P. Zhuang, *Phys. Rev. C* **89**, 054911 (2014).

[36] X. Du, R. Rapp, *Nucl. Phys. A* **943**, 147 (2015).

[37] M. He, B. Wu, R. Rapp, *Phys. Rev. Lett.* **128**, 162301 (2022).

[38] N. Brambilla *et al.*, *J. High Energy Phys.* **2021**, 136 (2021).

[39] X. Yao, *Int. J. Mod. Phys. A* **36**, 2130010 (2021).

[40] Y. Akamatsu, *Prog. Part. Nucl. Phys.* **123**, 103932 (2022).

[41] B. Krouppa, R. Ryblewski, M. Strickland, *Phys. Rev. C* **92**, 061901 (2015).

[42] X. Du, S.Y.F. Liu, R. Rapp, *Phys. Lett. B* **796**, 20 (2019).